Numerical cyclic behavior of T-RBS:
A new steel moment connection

Saeed Ataollahi [a], Mohammad-Reza Banan [*] and Mahmoud-Reza Banan [b]

Department of Civil and Environmental Engineering, Shiraz University, Shiraz, Iran

(*Received November 12, 2015, Revised May 21, 2016, Accepted August 06, 2016*)

Abstract. After observing relatively poor performance of bolted web-welded flange beam-to-column connections during 1994 Northridge earthquake, various types of connections based on two concepts of: (i) strengthening the connection; and (ii) weakening the beam ends were proposed. Among these modified or newly proposed connections, bolted T-stub connection follows the concept of strengthening. One of the connections with the idea of weakening the beam ends is reduced beam section (RBS). In this paper, finite element simulation is used to study the cyclic behavior of a new proposed connection developed by using a combination of both mentioned concepts. Investigated connections are exterior beam-to-column connections designed to comply with AISC provisions. The results show that moment capacity and dissipated energy of the new proposed connection is almost the same as those computed for a T-stub connection and higher than corresponding values for an RBS connection.

Keywords: cyclic behavior; steel moment connection; T-stub; beam-column connection; RBS

1. Introduction

Steel moment-frame buildings are designed to resist earthquake ground shaking based on the assumption that they are capable of extensive yielding and plastic deformation, without significant strength reduction and stiffness degradation (FEMA-350 2000).

The integrity of moment resisting frames lies largely on the ability of the connections to transmit moments and shear between the beams and columns (Gerami *et al.* 2011). Since the earthquakes of 1994 in Northridge and of 1995 in Kobe, intensive numerical and experimental research has been underway to find better methods to design and construct seismic resistant steel frames. A number of improved beam-to-column connection strategies have been proposed, which have shown to exhibit satisfactory levels of ductility in numerous tests. Two key concepts have been developed in order to provide highly ductile response and reliable performance for connections: strengthening the connection and weakening the beam framing into the connection, to avoid damages of the respective column.

The purpose of connection reinforcement is to provide a beam-to-column connection that is stronger than the connected beam section. The reinforcement is intended to force the plastic hinge

---

∗Corresponding author, Associate Professor, E-mail: banan@shirazu.ac.ir
[a] M.Sc., E-mail: saeedataollahi@gmail.com
[b] Ph.D., E-mail: bananm@shirazu.ac.ir

formation away from the face of the column, and also dictates large stresses and inelastic strains further into the beam. However, reinforcing the connection increases its cost and, if excessive reinforcement is used, may yield to very large weld sizes and higher degrees of restraint (Pachoumis *et al*. 2010). One of the connections with this philosophy of reinforcing is T-stub connection. Numerous experimental and numerical studies on behavior of this connection have been performed.

The other idea for improving a moment connection that provides advantages similar to reinforcement, and may avoid some of the disadvantages, is using the reduced beam section (RBS) connection.

The objective of this paper is to investigate the cyclic behavior of a new proposed connection composed of T-stub and RBS connection (hereafter will be called as T-RBS). This kind of connection has the advantage of eliminating the weld lines.

In recent years much research has been conducted to investigate the behaviors of T-stub and RBS connections individually. Some of these works are summarized as follows.

A series of tests were conducted by Swanson and Leon (2000) on 48 T-stub specimens in order to study the behavior, failure modes and ductility of T-stub connections. These tests were carried out as a part of a SAC phase II project. The results showed that the design relations are not necessarily good predictors for the governing failure modes.

A theoretical model for predicting the ultimate behavior of bolted T-stubs has been proposed by Piluso *et al*. (2001a) and Francavilla *et al*. (2016) and the first model validated by means of experimental tests (Piluso *et al*. 2001b).

Two exterior beam-to-column bolted T-stub connections were experimentally studied under cyclic loads by Popov and Takhirov (2002). One specimen had rectangular-shaped stem. The second specimen had U-shaped stem and bolts were located on the stem close to the fillet weld. The results demonstrated that the separation occurred between the T-stub flange and the column flange, had allowed energy dissipation and prevented severe buckling of the beam flange and beam web.

The use of bolted T-stubs equipped with friction dampers has been also recently proposed by Latour *et al*. (2015). The decoupling of stiffness and strength is obtained. The connection behaves as a partial strength connection where energy dissipation occurs in the friction dampers, thus preventing the damage to the connecting elements.

Coelho *et al*. (2004) experimentally investigated the behavior of 32 bolted T-stub connections. The research was mainly concentrated on the role of built-up T-stubs which were made by welded plates. The results showed that the welding procedure is particularly important to ensure a ductile behavior of the connection.

Piluso and Rizzano (2008) set up an experimental program devoted to the cyclic response of the most important components of bolted T-stub connections. The program was aimed at the modeling of the cyclic force-displacement curve of bolted T-stubs.

Through an experimental program and numerical analyses, Bravo and Herrera (2014) investigated that the failure modes and limit states which control the behavior of built-up T-stubs are the same that govern the hot rolled T-stub behavior.

A study was performed by Ricles *et al*. (2004) to investigate the effects of a floor slab on the seismic behavior of an interior moment connection between a pair of wide-flange steel beams and a deep column. This experimental program was conducted on six full-scale test specimens and results were compared with the corresponding results computed using finite element models.

An experimental analysis and finite element simulation were conducted by Pachoumis *et al*.

(2009) on two reduced beam section (RBS) moment resisting connections using the HEA profiles. The analyses confirmed the need for readjustment of the geometrical characteristics of the RBS in order to apply to the European profiles.

Numerical investigation was performed on seismic performance of rigid skewed beam-to-column connection with reduced beam section by *Zareia et al*. (2016).The results show that in addition to reverse twisting of columns, change in beam angle relative to the central axis of the column has little impact on hysteresis response of samples.

2. Scope

In this study, in order to develop a reliable numerical model for the proposed T-RBS connection, first two finite element models were individually constructed, one for T-stub connection and another one for RBS connection. Each model was calibrated against experimental results. Then a finite element model for T-RBS was developed such that it can reproduce the experimental results for T-stub and RBS connection, individually. After verification of the developed model for T-RBS, a reference model was designed and through a sensitivity analysis the numerical results obtained for moment-rotation and force-displacement curves as well as energy dissipation capacity were investigated.

3. Modeling method for verification

To evaluate the accuracy of the developed FE models for T-stub and RBS connections using ABAQUS package, the numerical results are compared with experimental results reported for specimen 1 for T-stub connection tested by Popov and Takhirov (2002) and for RBS connection the results of specimens tested by Pachoumis *et al*. (2010), respectively. The experimental specimens for both types of connections were single-sided beam-to-column assemblies that are representative of exterior beam-to-column connections.

For T-stub bolted connection, they used two T-sections that connect the beam flanges to column flange with high strength bolts. All the bolts were used in connecting the T-stem to the beam flange and T-flange to the column flange were pre-tensioned. To connect the beam web to the column flange a shear tab that was welded to the column flange and bolted to the beam web was used.

In the considered RBS connection, the beam is connected to the column flange by CJP weld. The numerical models of these connections are full-scale. All contacts between different surfaces are considered. Thus, the effect of adjacent contact surfaces' interaction, including T-stub steam/

Table 1 Material properties for T-stub connection

Connection element	Yield stress (MPa)	Ultimate stress (MPa)	Section profile
Beam	390	512.6	W36×150
Column	358.3	454.7	W14×283
T-stub	441	544.3	WT40×264
Bolt	890	1009	A490: $1''$, $1\frac{1''}{4}$

Table 2 Material properties for RBS connection

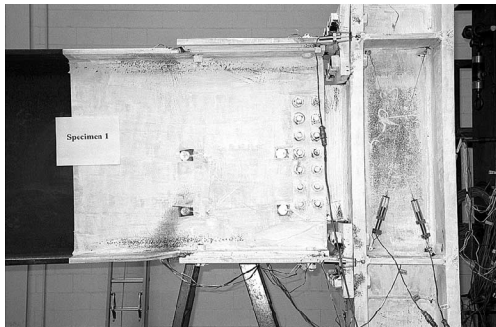| Connection element	Yield stress (MPa)	Ultimate stress (MPa)	Section size
Beam	310	430	HE 180A
Column	310	430	HE 300B
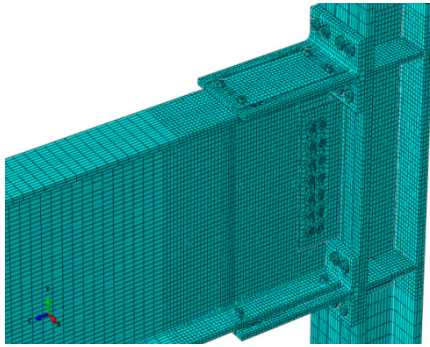
(a) T-stub
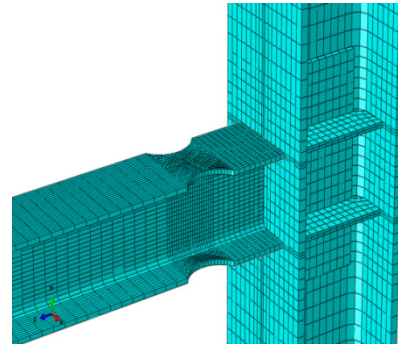
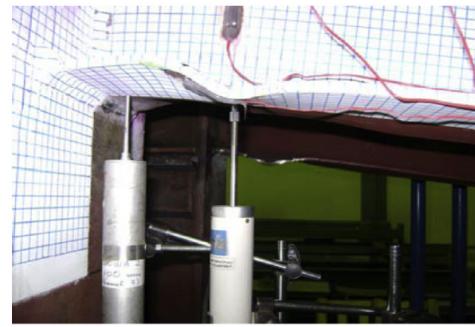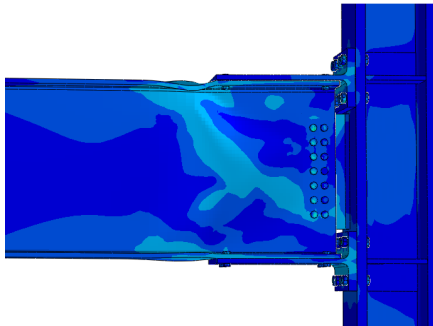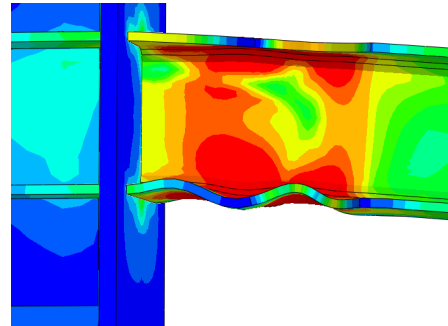(b) RBS

Fig. 1 Numerical models for the verified experimental specimens

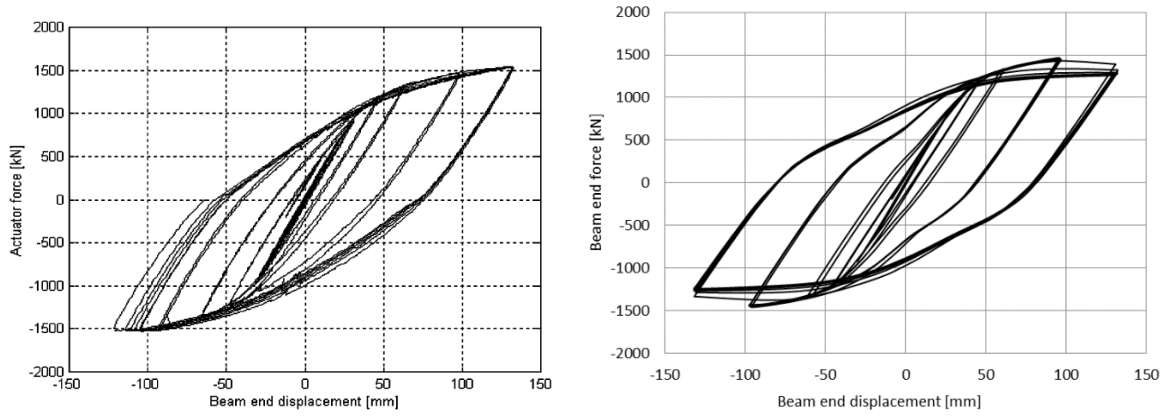(a) "Specimen1" after testing (Popov and Takhirov 2002)

(b) "Specimen RBSb" after testing (Pachoumis *et al*. 2010)

(c) FE model for "Specimen 1" after testing
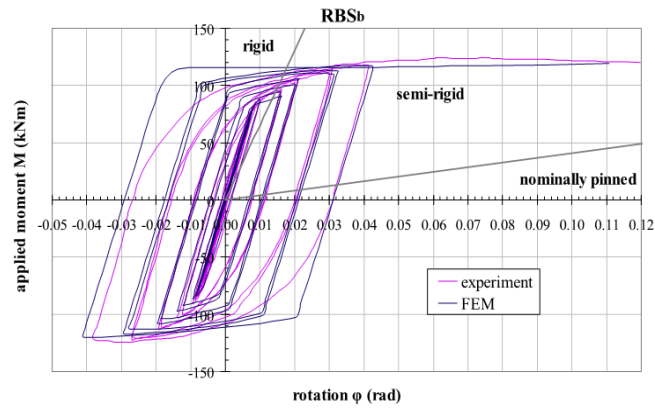

(d) FE model for "Specimen RBSb" after testing

Fig. 2 Overall behavior of experimental and numerical specimens

(a) Hysteresis curve for experimental T-stub
    specimen (Popov and Takhirov 2002)

(b) Hysteresis curve for numerical T-stub specimen

Fig. 3 Force-displacement hysteresis curves for experimental and numerical T-stub specimens

(a) Hysteresis curve for experimental and numerical RBS specimen (Pachoumis et al. 2010)
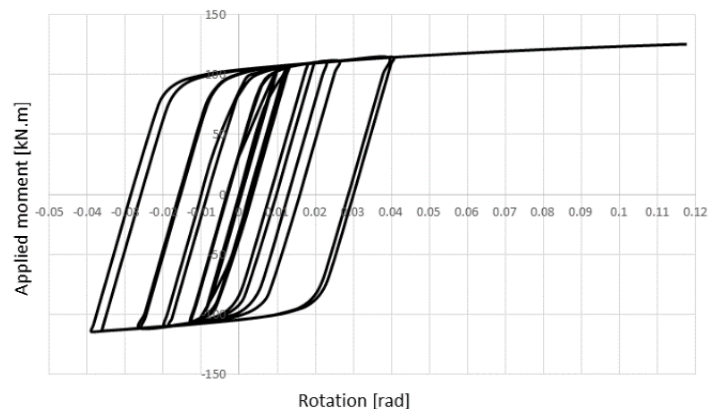
(b) Hysteresis curve for numerical RBS specimen

Fig. 4 Moment-rotation hysteresis curves for experimental and numerical RBS specimens

beam flange, T-stub flange/column flange, column flange/bolt head, T-stub flange/bolt nut and bolt hole/bolt shank and effect of friction are modeled. All connection models are constructed using C3D8R element (an 8-node linear brick with reduced integration and hourglass control).

The geometrical and mechanical properties of members making up each specimen are extracted from the experimental data which are summarized in Tables 1-2 for T-stub and RBS connections, respectively. To simulate plastic deformations of components involved in a connection, a bilinear-kinematic- hardening material behavior is used. This material model is suitable for simulation of metal plasticity under cyclic loading. In the simulation environment the load is applied in two steps. In the first step bolt pretension is applied and in the second step cyclic displacement is imposed.

To model pre-tension force in a bolt, a section is defined in the middle plane of the bolt and pre-tension load is applied to that plane. In each FE model, a rigid plate is connected to the beam end and cyclic displacement is applied to this rigid plate to prevent stress concentration at the tip of the beam.

Numerical models and finite element meshes for both types of connections are shown in Figs. 1(a)-(b). It can be seen from Figs. 2(a)-(d) that there is a good compatibility and correlation between the behavior of experimental and FE models. For the T-stub model plastic hinge is formed immediately after the stem tip with a slight buckling of flanges and web. For the RBS model plastic hinge is formed in the zone of reduced area of the beam flange. The comparison of experimental and FE cyclic curves for the T-stub connection which are reflected by the applied load versus tip displacement are shown in Fig. 3. Maximum applied load for experimental specimen is 1535 kN while for FE model, this value is 1456 kN, which shows a difference of 5%.

In Fig. 4, one can observe difference between various cyclic curves which plot the moment at the column face versus rotation at 750 mm from the column face for RBS connection. The maximum moment at the column face from experimental data is 121 kN.m while it is about 114 kN.m for FE model which gives a 5.8% difference.

4. Finite element models

The deflection as well as bending moment diagram of a moment resisting frame under lateral loads reveals that the bending moments at the midspans of the beam and the column are equal to zero. In other words, the midpoints of the beam and the column under lateral loads are the inflection points of the corresponding member. Unlike the bending moment, the value of the shear force at the inflection point is not equal to zero. Therefore; to focus on the behavior of the connection, a substructure bounded by inflection points in beams and columns is considered. The pinned or roller supports can be applied to bear the shear forces at end points and then the substructure can be modeled and analyzed as it is shown in Fig. 5.

The T-RBS connection models are single-sided beam-to-column assemblies that are representative of exterior connections. They are composed of 2-meter IPE450 beams and 3.5-meter IPB450 columns. These section profiles and dimensions are extracted from a designed 10-story building. Because of space limitation, design data is not provided here. For connection design, AISC requirements (Manual of steel construction 2005), (Kulak *et al.* 1987), (ANSI/AISC-358 2010) and (ANSI/AISC-360 2010) are followed. The T-stub member of the connection has flange thickness of 30 mm and stem thickness of 20 mm. The T-stem is connected to the beam flange with 10 M24, A490 bolts and a floating plate. The T-flange is connected to column flange
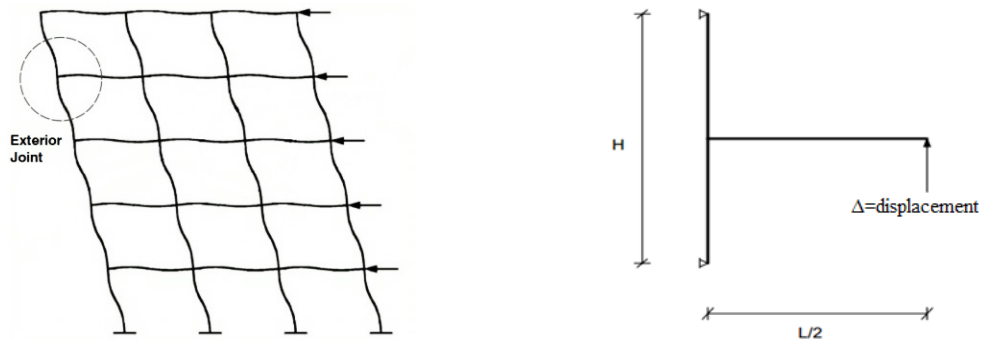
(a) Deformation of a moment frame subjected to lateral loads   (b) Substructure used in numerical study

Fig. 5 Substructure model for the joint area

with 8 M22, A490 bolts. A shear tab with 4 M24, A490 bolts connects the beam web to the column flange.

In RBS part of the connection, because of the presence of T-stub, dimension "a" is different from the allowable limits provided by AISC reference for connections (ANSI/AISC-358 2010). Details of the connection and 3D model are shown in Figs. 6-7, respectively.

Beams, columns and T-stub plates all are made of steel A572 Gr 50. The yielding and ultimate stresses used for each member are summarized in Table 3. To model the cyclic behavior of this specific material for nonlinear analysis, a bilinear-kinematic-hardening behavior is considered. The SAC standard loading protocol (SAC 2000) in accordance with (FEMA-350 2000) is applied to the specimen, as shown in Fig. 8 and presented in Table 4.
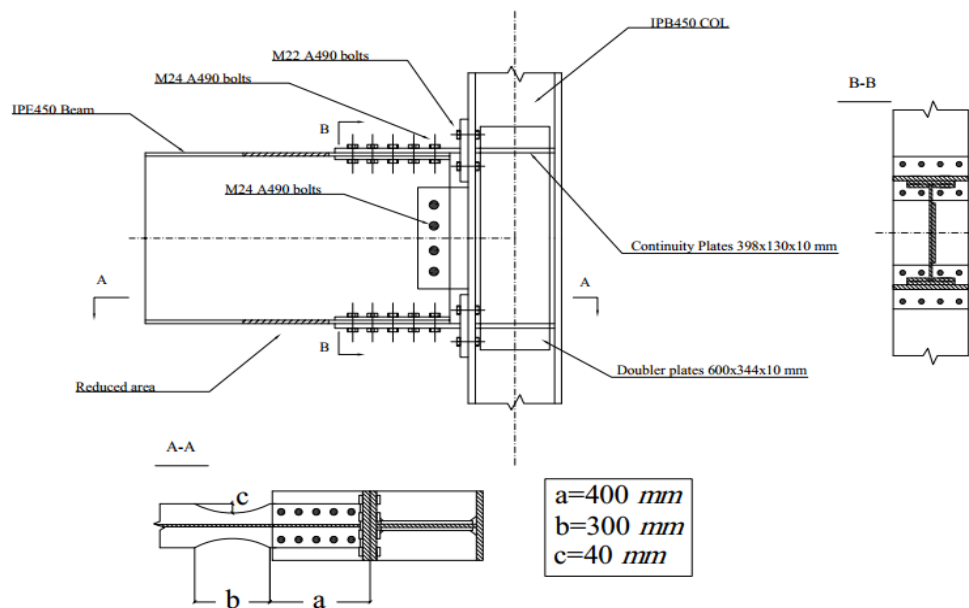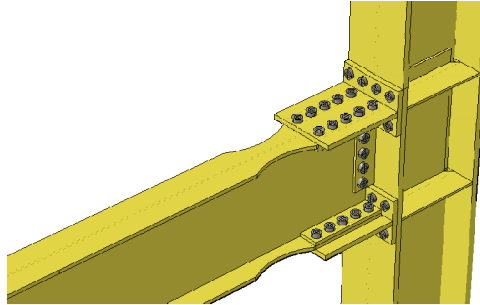

Fig. 6 Design details of T-RBS connection
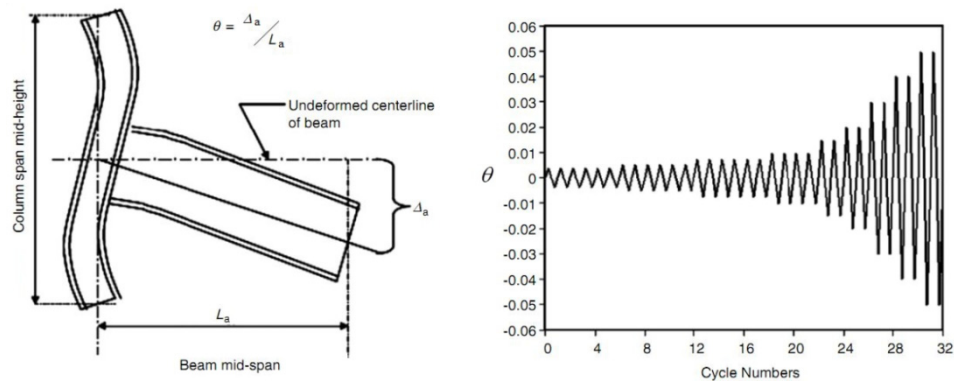
Fig. 7 A 3D model of T-RBS connection

Fig. 8 FEMA/SAC2000 loading protocol

Table 3 Material properties for T-RBS connection

Connection element	Yield stress (MPa)	Ultimate stress (MPa)	Section profile
Beam	345	450	IPE450
Column	345	450	IPB450
T-stub	345	450	
Bolt	890	1009	A490 M24, M22

Table 4 Details of cyclic loading protocol

Load step	Peak deformation, θ (rad)	Number of cycles
1	0.00375	6
2	0.00500	6
3	0.00750	6
4	0.01000	4
5	0.01500	2
6	0.02000	2
7	0.03000	2
8	0.04000	2
9	0.05000	2

5. Numerical results

To determine the main behaviors of a connection such as; force-displacement and moment-rotation curves, amount of dissipated energy and the initial stiffness, parameters like displacements, forces and stresses at some specific points of the connection assembly are recorded during the analysis. All the results for the T-RBS connection are compared with corresponding values computed for T-stub and RBS connections.

A mesh sensitivity analysis is initially performed to find an optimum mesh size. As a result, a more refined mesh is employed at the joint area. For the RBS area even a finer mesh with respect to the mesh defined in the joint area is used. The result of mesh study is shown in Fig. 9 and
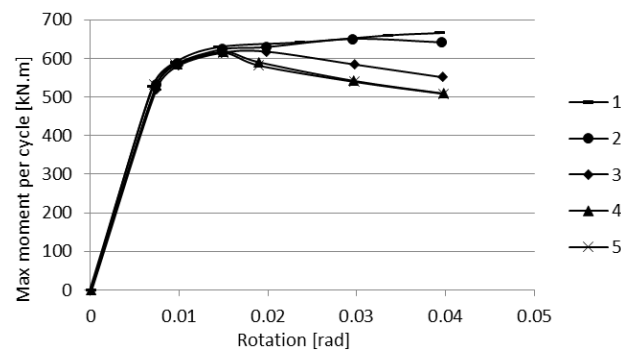

Fig. 9 Hysteresis envelope of moment vs. rotation for different sizes of mesh

Table 5 Amount of error for different sizes of mesh

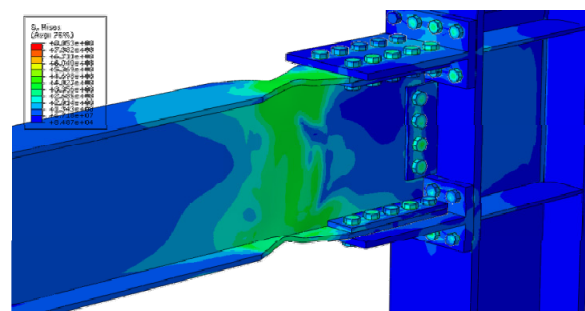| Mesh size	1 (0.1-0.05-0.03 m)*	2 (0.05-.025-0.25 m)	3 (0.05-0.025-0.015 m)	4 (0.05-0.025-0.01 m)	5 (0.04-0.02-0.01 m)
M_u (kN.m) at 0.04 rad	666	641.8	551.4	509.2	508.2
Error with respect to curve No. 5 (%)	23.7	20.8	7.8	0.2	-

Fig. 10 Von-Mises stress of the connection at the end of the analysis

Table 5. The difference between curves No. 1 through 5 is the mesh size employed in three above-mentioned zones. The numbers in parentheses are representation of mesh size for (beam and column, joint area and RBS area, respectively). For example in curve No. 1, the mesh size for beam and column, joint area and RBS area are 0.1, 0.05, 0.03 m, respectively. Since curves No. 4 and No. 5 are almost the same, we will use dimensions associated with curve No. 4.

It is observed that first yielding was initiated at the flanges of the beam in the RBS area and then accompanied by buckling of the beam web at the RBS area. A close-up side view of the specimen with contours representing Von-Mises stress at the end of the analysis is presented in Fig. 10. The cyclic curves showing variations of load versus displacement, moment at the column centerline versus rotation and moment versus plastic rotation are presented in Figs. 11-13, respectively. Plastic rotation is defined as the total rotation minus elastic rotation.

Table 6 summarizes the detailed results for the maximum moment that a connection could resist, the moment and dissipated energy at 0.04 *rad* rotation, and the initial stiffness of the considered connections. Computed parameters for joints with either RBS or T-stub connection are presented and compared with corresponding values from T-RBS connection. Backbones of moment-rotation curves for these three types of connections are plotted in Fig. 14.

It can be seen (from Fig. 10) that the failure occurs by plastic hinge formation in the RBS area. By comparing numerical results in Table 6, one can conclude that the maximum moment in T-RBS connection is reduced by 25% compared with T-stub connection, and is increased by 15% compared with RBS connection. Dissipated energy at rotation of 0.04 *rad* in T-RBS connection is
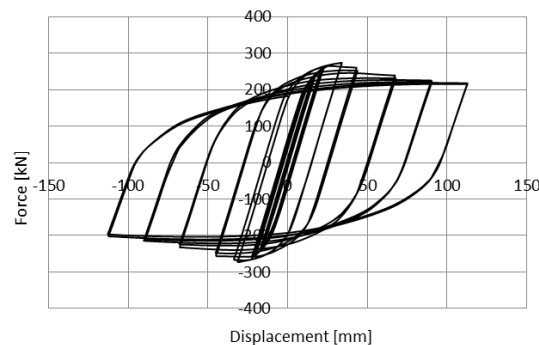

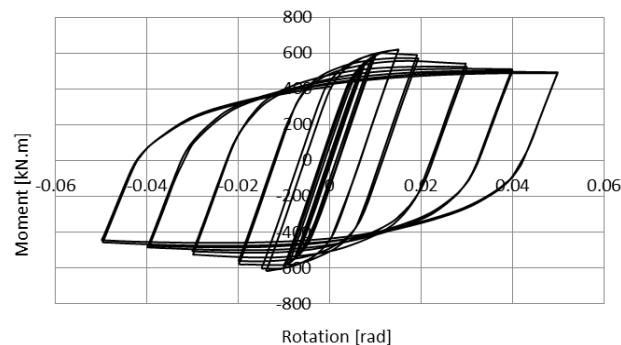Fig. 11 Hysteresis curve of force Vs. displacement

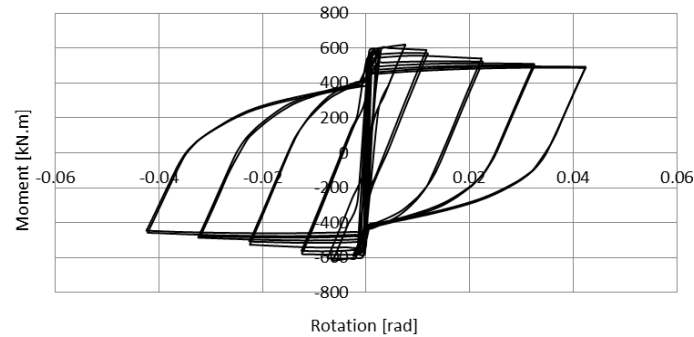Fig. 12 Hysteresis curve of Moment Vs. rotation

Fig. 13 Hysteresis curve of Moment Vs. plastic rotation

Table 6 Comparison of basic parameters computed for T-RBS, T-stub, RBS connections

Connection type	M_{max} (kN.m)	$M_{0.04rad}$ (kN.m)	Energy (N.m)[*]	K_i (10^6 N/m)[**]
T-RBS	617	515	60331	13.95
T-stub	824	810	81541	14.19
RBS	536	393	42662	12.1

* Dissipated energy at 0.04 *rad* rotation
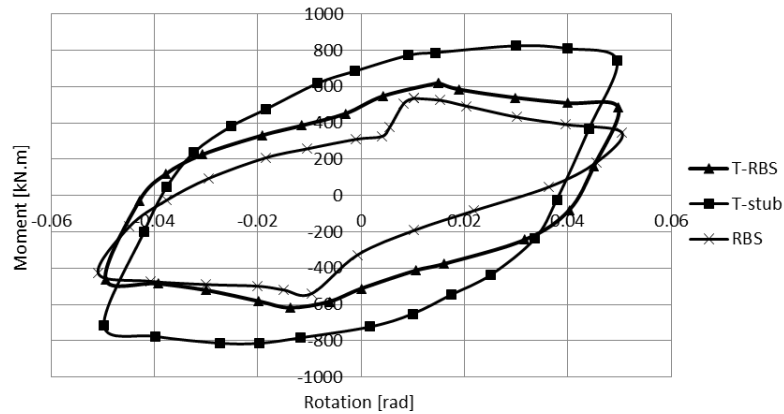** Initial stiffness

Fig. 14 Backbones of moment-rotation curves for T-RBS, T-stub and RBS connection

reduced by 25% compared with T-stub connection, and is increased by 41% compared with RBS connection.

The normalized cyclic curve of moment at the column face towards plastic moment versus rotation is presented in Fig. 15. The ratio of moment at column face over plastic moment for T-RBS connection at the rotation of 0.04 *rad*, is 0.75. The ratio of moment at the RBS area over plastic moment at the rotation of 0.04 *rad*, is 0.79. This ratio for a prequalified connection should be 0.8, but since the RBS area prevents large demands at the column face, this criterion may not be a good parameter to quantify the behavior of this kind of connection and consequently qualifying the connection.
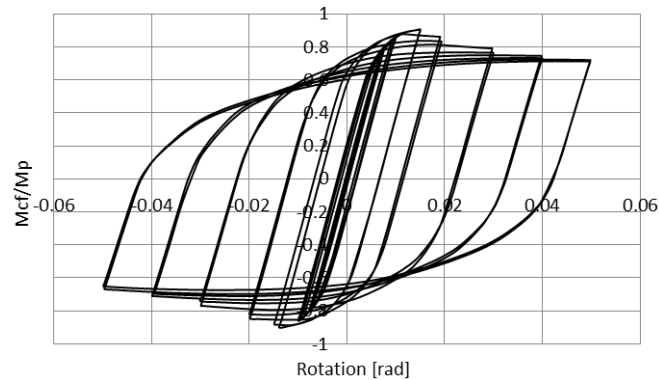
Fig. 15 Hysteresis curve of Moment at column face Vs. rotation

5.1 The effect of T-stub flange thickness

One significant behavioral characteristic of all bolted connections is prying action. Prying action refers to secondary forces that are introduced to the tension bolts in addition to the expected or conventional tension. For this reason, in design of T-stub connections there is limitation for T-stub flange thickness to prevent prying action. With presence of RBS area in T-RBS connection, there is less demand at the column face and also at T-stub flange zones. The minimum allowable flange thickness for T-stub according to design specification is 30 mm for this connection. In this paper, the flange thickness of T-stub is reduced and modeled and analyzed for the purpose of
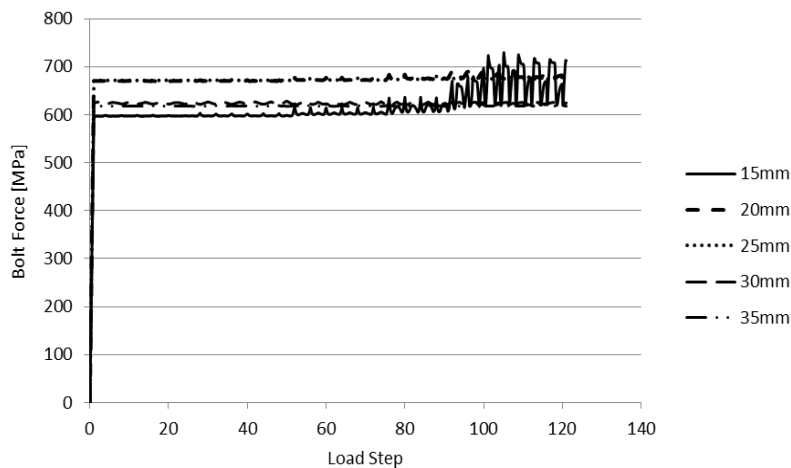

Fig. 16 Bolt stress during the loading

Table 7 Max stress in critical bolt

T-stub flange thickness (mm)	15	20	25	30	35
Max M22 bolt stress (MPa)	729.7	690.3	682.2	628.5	626.1

parametric study. In Fig. 16 the stress in most critical bolt in T-stub flange for different sizes of flange thickness is presented, and results are summarized in Table 7. One can observe from the curves presented in Fig. 16 and the results listed in Table 7, that the case with 15 mm flange thickness is in a critical condition and causes the critical bolt to reach its tensile capacity which means bolt failure. In other cases the critical bolt is in a stable condition and reducing the flange thickness does not significantly affect the T-stub capacity.

6. Conclusions

In this paper the cyclic behavior of a newly proposed connection called T-RBS is investigated using finite element analysis. A summary of conclusions are listed as follows:

- The failure is occurred by the formation of a plastic hinge in the beam at the RBS area. Yielding initiated at the flanges of the beam at the RBS area and then accompanied by buckling of the beam web in the RBS area.
- The maximum moment in T-RBS connection is reduced by 25% compared with corresponding value for T-stub connection, and is increased by 15% when compared with maximum moment in RBS connection.
- Dissipated energy at rotation of 0.04 *rad* in T-RBS connection is reduced by 25% compared with T-stub connection, and is increased by 41% compared with RBS connection.
- The ratio of moment at column face over plastic moment for T-RBS connection is 0.75, also the ratio of moment at the RBS area over plastic moment is 0.79.
- Because of the presence of RBS area, there is less demand on the T-stub flange. For this reason, the T-stub flange thickness can be reduced. It is recommended that the AISC specification for preventing prying action be modified for this new connection.

References

ABAQUS/PRE (1997), User's Manual, Hibbit, Karlsson and Sorensen Inc.

AISC (2005), Manual of Steel Construction, (13th Ed.), American Institute of Steel Construction, Chicago, IL, USA.

ANSI/AISC 358-10 (2010), Prequalified connections for special and intermediate steel moment frames for seismic applications; American Institute of Steel Construction, Chicago, IL, USA.

ANSI/AISC 360-10 (2010), Specification for structural steel buildings; American Institute of Steel Construction, Chicago, IL, USA.

Bravo, M.A. and Herrera, R.A. (2014), "Performance under cyclic load of built-up T-stubs for Double T moment connections", *Constructional Steel*, **103**, 117-130.

Coelho, A.G., Bijlaard, F.K., Gresnigt, N. and Simoes da Silva, L. (2004), "Experimental assessment of the behaviour of bolted T-stub connections made up of welded plates", *Constructional Steel*, **60**(2), 269-311.

FEMA-350 (2000), *Recommended Seismic Design Criteria for New Steel Moment-Frame Buildings*, Federal Emergency Management Agency, Washington D.C., USA.

Francavilla, A.B., Latour, M., Piluso, V. and Rizzano, G. (2016), "Bolted T-stubs: A refined model for flange and bolt fracture modes", *Steel Compos. Struct., Int. J.*, **20**(2), 267-293.

Gerami, M., Saberi, H., Saberi, V. and Saedi Daryan, A. (2011), "Cyclic behavior of bolted connections with different arrangement of bolts", *Constructional Steel*, **67**(4), 690-705.

Kulak, G.L., Fisher, J.W. and Struik, J.H. (1987), *Guide to Design Criteria for Bolted and Riveted Joints*,

AISC, Chicago, IL, USA.

Latour, M., Piluso, V. and Rizzano, G. (2015), "Free from damage beam-to-column joints: Testing and design of DST connections with friction pads", *Eng. Struct.*, **85**, 219-233.

Pachoumis, D.T., Galoussis, E.G., Kalfas, C.N. and Christitsas, A.D. (2009), "Reduced beam section moment connections subjected to cyclic loading: Experimental analysis and FEM simulation", *Eng. Struct.*, **31**(1), 216-223.

Pachoumis, D.T., Galoussis, E.G., Kalfas, C.N. and Efthimiou, I.Z. (2010), "Cyclic performance of steel moment-resisting connections with reduced beam sections − Experimental analysis and finite element model simulation", *Eng. Struct.*, **32**(9), 2683-2692.

Piluso, V., Faella, C. and Rizzano, G. (2001a), "Ultimate behavior of bolted T-stubs - I. Theoretical model", *J. Struct. Eng.*, **127**(6), 686-693.

Piluso, V., Faella, C. and Rizzano, G. (2001b), "Ultimate behavior of bolted T-stubs - II. Model validation", *J. Struct. Eng.*, **127**(6), 694-704.

Piluso, V. and Rizzano, G. (2008), "Experimental analysis and modeling of bolted T-stubs under cyclic loads", *Constructional Steel*, **64**(6), 655-669.

Popov, E. and Takhirov, S. (2002), "Bolted large seismic steel beam-to-column connections, part 1: experimental study", *Eng. Struct.*, **24**(12), 1523-1534.

Ricles, J.M., Zhang, X., Lu, L.W. and Fisher, J. (2004), Development of Seismic Guidelines for Deep-Column Steel Moment Connections, (ATLSS Report No. 04-13), National Center for Engineering Research on Advanced Technology for Large Structural Systems, Bethlehem, PA, USA.

SAC (2000), Seismic design criteria for new moment-resisting steel frame construction; FEMA 350, SAC Joint Venture, Sacramento, CA, USA.

Swanson, J.A. and Leon, R.T. (2000), "Bolted steel connection: Tests on T-stub components", *J. Struct. Eng.*, **126**(1), 50-60.

Zareia, A., Vaghefi, M. and Fiouz, A.R. (2016), "Numerical investigation seismic performance of rigid skewed beam-to-column connection with reduced beam section", *Struct. Eng. Mech., Int. J.*, **57**(3), 507-528.

CC